Inorganic Chemistry

Article

pubs.acs.org/IC

Selective DNA Purine Base Photooxidation by Bis-terdentate Iridium(III) Polypyridyl and Cyclometalated Complexes

Alexandre Jacques, Andrée Kirsch-De Mesmaeker,† and Benjamin Elias*

Institut de la Matière Condensée et des Nanosciences, Université Catholique de Louvain, Place Louis Pasteur 2, Box L4.01.02, B-1348 Louvain-la-Neuve, Belgium

Supporting Information

ABSTRACT: Two bis-terdentate iridium(III) complexes with polypyridyl and cyclometalated ligands have been prepared and characterized. Their spectroscopic and electrochemical properties have been studied, and a photophysical scheme addressing their properties is proposed. Different types of excited states have been considered to account for the deactivation processes in each complex. Interestingly, in the presence of mono- or polynucleotides, a photoinduced electron-transfer process from a DNA purine base (i.e., guanine or adenine) to the excited complex is shown through luminescence quenching experiments. For the first time, this work reports evidence for selective DNA purine bases oxidation by excited iridium(III) bis-terdentate complexes.

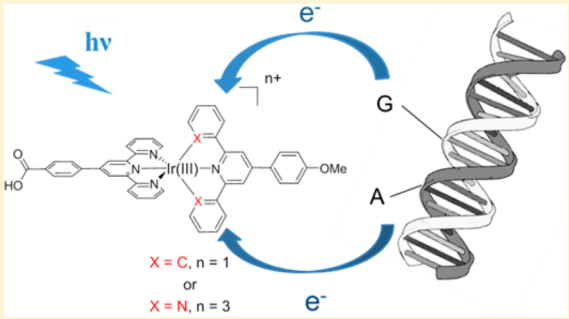

INTRODUCTION

Polyazaaromatic transition-metal complexes have gained considerable interest these past decades. Their use as catalysts in the water splitting process,[1] therapeutic agents in several cancer treatments,[2] or photoprobes of biological media[3] is well-established. Among all transition metals available, iridium(III) is one of the most interesting elements for building complexes.[4] Indeed, it allows the synthesis of multiple polypyridyl and cyclometalated complexes with bidentate or terdentate ligands. Iridium(III) is capable of forming stable mono-, bis-, and tris-cyclometalated complexes, and up to three C-donor sites can be coordinated onto the metal center. The C/N ratio present in the first coordination sphere can thus be varied from 0/6 to 3/3, hence providing an excellent means to tune the photoredox properties of the resulting complexes. For instance, tris-bidentate iridium(III) complexes made of two PPY (PPY = 2-phenylpyridine) and an imidazo[4,5-*f*][1,10]phenanthroline have C/N = 2/4 and are specific anion sensors.[5] Upon replacement of the imidazolo ligand by an intercalative ligand dppz (dppz = dipyrido[3,2-*a*:2′,3′-*c*]phenazine), the resulting luminescent iridium(III) has been used to study DNA-mediated hole and electron transfer.[6] Recently, it has been shown that a luminescent bis-terdentate iridium(III) complex made exclusively of terpyridine-type-like ligands (C/N = 0/6) exhibits intercalation between DNA base pairs.[7] The luminescence of this complex is quenched in the presence of a guanine moiety via a photoinduced electron-transfer process, showing the high oxidizing ability of the excited state. Although displaying spectroelectrochemical properties enabling photoreactions toward DNA, iridium(III) complexes have only been scarcely used as such in the literature. Therefore, in this paper, we present the comprehensive study of two novel iridium(III) complexes obtained from the coordination of either two terpyridyl-like ligands {i.e., [Ir(4′-COOH-Phtpy)(4′-MeO-Phtpy)]$^{3+}$ [4′-COOH-Phtpy = 4′-(4-carboxyphenyl)-2,2′:6′,2″-terpyridine and 4′-MeO-Phtpy = 4′-(4-methoxyphenyl)-2,2′:6′,2″-terpyridine] called hereafter [**IrN$_6$**]$^{3+}$ for the sake of clarity; Figure 1} or one terpyridyl and one triphenylpyridyl ligands {i.e., [Ir(4′-COOH-Phtpy)(4′-MeO-tppy)]$^{+}$ [4′-MeO-tppy = 2,6-diphenyl-4-(4′-methoxyphenyl)pyridine] called hereafter [**IrN$_4$C$_2$**]$^{+}$ for the sake of clarity; Figure 1}. Their photophysics and photochemistry have been investigated. Although both complexes display very similar structural features, their photoredox behavior toward DNA bases and the excited state involved in the electron transfer process are quite different depending on the coordination sphere. Using luminescence measurements in the absence and presence of several DNA building blocks, synthetic or natural DNA, we were able to show that these complexes selectively photooxidize purine nucleobases (i.e., adenine and guanine), whereas no nucleobase reduction occurs under irradiation. This paper represents, to the best of our knowledge, one of the very few studies addressing photoinduced electron-transfer processes between excited bis-terdentate iridium(III) complexes and DNA bases.

EXPERIMENTAL SECTION

Materials and Instrumentation. 4′-(Methoxyphenyl)-2,2′:6′,2″-terpyridine[8] (4′-MeO-Phtpy), [(4′-COOMe-Phtpy)IrCl$_3$],[9] [(4′-COOH-Phtpy)IrCl$_3$],[10] and 2,6-diphenyl-4-(4′-methoxyphenyl)-pyridine[11] (4′-MeO-tppy) were prepared as previously described. Deoxynucleotides (dGMP, dAMP, dCMP, and dTMP) were

Received: October 1, 2013
Published: January 22, 2014

   dx.doi.org/10.1021/ic402476b | *Inorg. Chem.* 2014, 53, 1507−1512

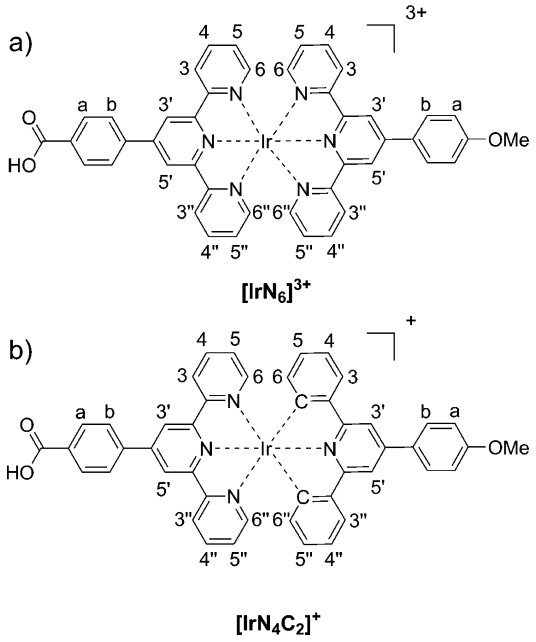

Figure 1. Structures of the iridium(III) complexes: (a) $[\mathbf{IrN_6}]^{3+}$; (b) $[\mathbf{IrN_4C_2}]^{+}$.

purchased from Sigma-Aldrich (purity ≥99%) and used without further purification. Calf thymus DNA (CT-DNA) was purchased from Sigma-Aldrich, and [poly(dG-dC)]$_2$, [poly(dA-dT)]$_2$, and [poly(dA)-poly(dT)] were purchased from Amersham Bioscience. Polynucleotide phosphate concentrations were determined spectroscopically ($\varepsilon_{260\ nm}$ = 6600 M^{-1} for CT-DNA,[12] $\varepsilon_{262\ nm}$ = 6600 M^{-1} for [poly(dA-dT)]$_2$,[13] $\varepsilon_{260\ nm}$ = 6000 M^{-1} for [poly(dA)-poly(dT)],[14] and $\varepsilon_{254\ nm}$ = 8400 M^{-1} for [poly(dG-dC)]$_2$).[15] ^{1}H NMR experiments were performed in CD_3CN on a Bruker AC-300 Avance II (300 MHz) or on a Bruker AM-500 (500 MHz). The chemical shifts (given in ppm) were measured versus the residual peak of the solvent as the internal standard. High-resolution mass spectrometry (HRMS) were recorded on a Q-Extractive orbitrap from ThermoFisher. Samples were ionized by electrospray ionization (ESI; capillary temperature = 250 °C, vaporizer temperature = 250 °C, sheath gas flow rate = 20). UV−vis absorption spectra were recorded on a Shimadzu UV-1700. Room temperature fluorescence spectra were recorded on a Varian Cary Eclipse instrument. Luminescence lifetimes were measured with a modified Applied Photophysics laser kinetic spectrometer by exciting the samples at 355 nm with a Nd:YAG pulsed laser (Continuum NY 61-10). Emitted light as a function of time was detected with a R-928 Hamamatsu photomultiplier tube whose output was applied to a digital oscilloscope (Hewlett-Packard HP 54200A) interfaced with a Dell Dimension DE051 computer. Signals were averaged over at least 16 shots and corrected for baseline. *Igor 6.1* software was used for decay analyses. Cyclic voltammetry was carried out in a one-compartment cell, using a glassy carbon disk working electrode (approximate area = 0.03 cm^2), a platinum wire counter electrode, and an Ag/AgCl reference electrode. The potential of the working electrode was controlled by an Autolab PGSTAT 100 potentiostat through a PC interface. The cyclic voltammograms were recorded with a sweep rate of 100 mV s^{-1}, either in dried acetonitrile (Acros, HPLC grade) or in dried *N*,*N*-dimethylformamide (DMF; Sigma-Aldrich, HPLC grade). Tetrabutylammonium perchlorate (0.1 M) was used as the supporting electrolyte, and the samples were purged by argon before each measurement.

[Ir(4′-COOH-Phtpy)(4′-MeO-Phtpy)](PF$_6$)$_3$ ([IrN$_6$](PF$_6$)$_3$). A suspension of [(4′-COOH-Phtpy)IrCl$_3$] (24 mg, 0.037 mmol) and 4′-MeO-Phtpy (12 mg, 0.037 mmol) was heated to 170 °C in degassed ethylene glycol (2.5 mL) in the dark and under argon for 30 min. After cooling, aqueous NH_4PF_6 was added to precipitate the crude product. The pure complex was isolated by column chromatography on Al_2O_3 (acetone/water, from 100/0 to 90/10), which yielded the complex $[\mathbf{IrN_6}]^{3+}$ (PF_6^- salt) as a yellow solid (40 mg, 82%). When the chloride salt was required for the experiments, counteranion exchange was achieved upon the addition of $^tBu_4N^+Cl^-$ to the PF_6^- salt dissolved in acetone. ^{1}H NMR (CD_3CN, 500 MHz): δ 9.11 (s, 2H, H_3' and H_5' of tpy-C_6H_4-COOH), 9.03 (s, 2H, H_3' and H_5' of tpy-C_6H_4-OMe), 8.72 (d, 2H, H_3 and H_3'' of tpy-C_6H_4-COOH, J_{H3-H4} = 8.1 Hz), 8.70 (d, 2H, H_3 and H_3'' of tpy-C_6H_4-OMe, J_{H3-H4} = 8.1 Hz), 8.40 (d, 2H, H_a of tpy-C_6H_4-COOH, J_{Ha-Hb} = 8.4 Hz), 8.28 (d, 2H, H_b of tpy-C_6H_4-COOH, J_{Hb-Ha} = 8.4 Hz), 8.25−8.20 (m, 6H, H_4 and H_4'' of both tpy's, H_b of tpy-C_6H_4-OMe), 7.70 (dd, 2H, H_6 and H_6'' of tpy-C_6H_4-OMe, J_{H6-H5} = 4.9 Hz, J_{H6-H4} = 0.9 Hz), 7.68 (dd, 2H, H_6 and H_6'' of tpy-C_6H_4-OMe, J_{H6-H5} = 4.9 Hz, J_{H6-H4} = 0.9 Hz), 7.51−7.46 (m, 4H, H_5 and H_5'' of both tpy's), 7.34 (d, 2H, H_a of tpy-C_6H_4-COOH, J_{Ha-Hb} = 8.8 Hz), 3.99 (s, 3H, OMe). HRMS (ESI). Calcd for $[C_{44}H_{32}N_6O_3{}^{193}IrP_2F_{12} - PF_6]^+$: *m*/*z* 1175.1443. Found: *m*/*z* 1175.1429. Calcd for $[C_{44}H_{32}N_6O_3{}^{193}Ir - 3PF_6]^{3+}$: *m*/*z* 295.0716. Found: *m*/*z* 295.0723.

[Ir(4′-COOH-Phtpy)(4′-MeO-tppy)](NO$_3$)$_3$ ([IrN$_4$C$_2$](NO$_3$)). A mixture of [(4′-COOMe-Phtpy)IrCl$_3$] (98 mg, 0.15 mmol), 4′-MeO-tppy (54 mg, 0.16 mmol), and $AgNO_3$ (125 mg, 0.74 mmol) was refluxed in degassed ethylene glycol (13 mL) in the dark and under argon for 22 h. After cooling, the mixture was filtered through Celite to remove AgCl. The Celite was washed with MeOH and subsequently evaporated. Water was added, and the aqueous layer was extracted with $CHCl_3$ (three times). The organic solutions were combined and evaporated to dryness. The crude product was purified by column chromatography on SiO_2 [CH_3CN/saturated aqueous KNO_3 (10/1)]. The first eluted orange band was recovered and the solvent evaporated. The resulting red solid was saponified in a mixture MeOH (30 mL)/1 M NaOH (20 mL), and the solution was heated to 80 °C for 3 h. After cooling, the solution was adjusted to pH = 7 with 2 M HCl and solvents were evaporated. The solid was purified by column chromatography on SiO_2 [CH_3CN/saturated aqueous KNO_3 (10/1)]. The red powder was washed with water and dried under vacuum to afford $[\mathbf{IrN_4C_2}]^+$ with 40% yield (63 mg). ^{1}H NMR (CD_3CN, 300 MHz): δ 9.00 (s, 2H, H_3' and H_5' of tpy-C_6H_4-COOH), 8.67 (d, 2H, H_3 and H_3'' of tpy-C_6H_4-COOH, J_{H3-H4} = 7.8 Hz), 8.36 (d, 2H, H_a of tpy-C_6H_4-COOH, J_{Ha-Hb} = 8.6 Hz), 8.29 (s, 2H, H_3' and H_5' of tppy-OMe), 8.28 (d, 2H, H_b of tpy-C_6H_4-COOH, J_{Hb-Ha} = 8.6 Hz), 8.13 (d, 2H, H_b of tppy-OMe, J_{Hb-Ha} = 8.4 Hz), 8.03−7.96 (m, 4H, H_4 and H_4'' of tpy-C_6H_4-COOH and H_3 and H_3'' of tppy-OMe), 7.89 (d, 2H, H_6 and H_6'' of tpy-C_6H_4-COOH, J_{H6-H5} = 5.1 Hz), 7.31−7.24 (m, 4H, H_5 and H_5'' of tpy-C_6H_4-COOH and H_a of tppy-OMe), 7.01 (td, 2H, H_4 and H_4'' of tppy-OMe, $J_{H4-H5\ (H3)}$ = 7.4 Hz, J_{H4-H6} = 1.1 Hz), 6.78 (td, 2H, H_5 and H_5'' of tppy-OMe, $J_{H5-H4\ (H6)}$ = 7.3 Hz, J_{H5-H3} = 1.0 Hz), 6.28 (dd, 2H, H_6 and H_6'' of tppy-OMe, J_{H6-H5} = 7.3 Hz, J_{H6-H4} = 0.9 Hz), 3.97 (s, 3H, OMe). HRMS (ESI). Calcd for $[C_{46}H_{32}N_4O_3{}^{193}Ir - NO_3]^+$: *m*/*z* 881.2098. Found: *m*/*z* 881.2088.

RESULTS

Synthesis. The synthesis of both complexes was achieved in two steps by heating iridium(III) chloride salts with the desired ligand in ethylene glycol according to methodologies previously described.[9,16] It is worth mentioning that the synthesis of $[\mathbf{IrN_4C_2}]^+$ requires harsher conditions than that of $[\mathbf{IrN_6}]^{3+}$, as expected from the greater inertness of the cyclometalated ligand. $[\mathbf{IrN_6}]^{3+}$ and $[\mathbf{IrN_4C_2}]^+$ display very similar structural features. Thanks to the derivatization on the 4′ position, they have several symmetry elements, hence circumventing the problem of the occurrence of geometrical isomers as encountered for tris-bidentate arrangements. Both complexes have thus been unambiguously characterized by ^{1}H NMR spectroscopy and HRMS (see the Experimental Section).

Electrochemistry. The redox potentials of both complexes were determined by cyclic voltammetry measurements. The data are gathered in Table 1. $[\mathbf{IrN_6}]^{3+}$ displays two irreversible

dx.doi.org/10.1021/ic402476b | *Inorg. Chem.* 2014, 53, 1507−1512

Table 1. Electrochemical Data Measured at Room Temperature in DMF for $[IrN_6]^{3+}$ and in CH_3CN for $[IrN_4C_2]^+$ with 0.1 M Bu_4NClO_4 as the Supporting Electrolyte[a]

	$[IrN_6]^{3+}$	$[IrN_4C_2]^+$
E_{ox} (V vs Ag/AgCl)	>2.2	1.14 (r, ΔE_p = 58 mV)
E_{red} (V vs Ag/AgCl)	−0.81 (ir), −1.22 (ir)	−1.24 (r, ΔE_p = 54 mV)
E_{ox}* (V vs Ag/AgCl)		−1.22
E_{red}* (V vs Ag/AgCl)	1.38	1.12

[a] r = reversible; ir = irreversible; ΔE_p (the peak-to-peak separation) is close to 59 mV.

one-electron-reduction waves at −0.81 and −1.22 V vs Ag/AgCl (Figure S1 in the SI). No oxidation process could be detected up to +2.2 V vs Ag/AgCl, suggesting that the oxidation is highly energetic and probably metal-centered. In contrast, $[IrN_4C_2]^+$ is characterized by one reversible reduction wave and one reversible oxidation wave, at −1.24 and +1.14 V vs Ag/AgCl, respectively (Figures S2 and S3 in the SI). The oxidation of $[IrN_4C_2]^+$ is probably due to the cyclometalated iridium fragment (Ir−C^N^C). The potentials in the excited state (namely, E_{ox}* and E_{red}*)[17] for both complexes have been estimated from the ground-state redox potentials and the energy of the excited state corresponding to the maximum of the emission spectrum at 298 K, i.e., $\lambda_{max\ Em}$ = 568 nm (2.19 eV) for $[IrN_6]^{3+}$ and $\lambda_{max\ Em}$ = 528 nm (2.36 eV) for $[IrN_4C_2]^+$. Not surprisingly, $[IrN_6]^{3+}$ is strongly oxidizing (E_{red}* = +1.38 V vs Ag/AgCl) in its excited state.

Absorption and Emission Spectroscopy. Absorption and emission spectra in CH_3CN under air at room temperature for both complexes are shown in Figure 2. Table 2 gathers the corresponding data. For both complexes, absorption (ε > 30000 M^{-1} cm^{-1}) bands in the UV region tailing into the visible are observed.

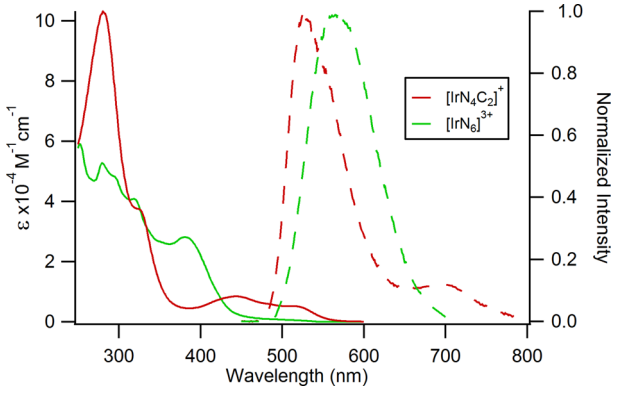

Figure 2. Absorption (solid lines) and emission (dashed lines; λ_{exc} = 350 nm) for $[IrN_6]^{3+}$ (green) and $[IrN_4C_2]^+$ (red) complexes in CH_3CN under air at room temperature.

$[IrN_6]^{3+}$ and $[IrN_4C_2]^+$ emit in CH_3CN under air ($\Phi \sim 10^{-3}$). A broad-band emission centered at around 568 nm ($\tau_{RT,air}$ = 470 ns) is observed for $[IrN_6]^{3+}$, whereas $[IrN_4C_2]^+$ exhibits a dual-band emission, centered at 528 nm ($\tau_{RT,air}$ = 1 μs) and 697 nm ($\tau_{RT,air}$ = 260 ns). Although there is almost no emission band shift between CH_3CN and water, the excited-state lifetimes are affected upon solvent change and increase by a factor of 2 or 3 in water for both complexes. It is worth mentioning that, in an air-equilibrated solvent, a decrease in the luminescence intensity with respect to degassed solutions is observed, showing a sensitization of $^1O_2$ by excited iridium(III) complexes. Because all of our experiments have been carried out under the same conditions, the influence of oxygen is kept constant and is therefore not further investigated in the present manuscript.

Table 2. Absorption and Luminescence Data for the Iridium(III) Complexes

		$[IrN_6]^{3+}$	$[IrN_4C_2]^+$	
$\lambda_{max\ Abs}$, nm (ε, ×10^{-3} M^{-1} cm^{-1})	CH_3CN	382 (28.1), 319 (40.8), 279 (52.7), 252 (59.0)	512 (5.2), 439 (8.4), 325 (37.4), 281 (102.8)	
$\lambda_{max\ Em}$[a] (nm) under air at 298 K	CH_3CN	568	528	697
	H_2O[b]	560	514	682
$\lambda_{max\ Em}$[a] (nm) at 77 K	EtOH/MeOH (4/1)	505	505	663
τ (μs) under air at 298 K	CH_3CN	0.47	1.00	0.26
	H_2O[b]	1.31	1.76	0.39
Φ[c]	CH_3CN	0.0010	0.0055	0.0006
	H_2O[b]	0.0019	0.0291	0.0227
k_r (×10^{-3} s^{-1})[d]	CH_3CN	2.2	5.5	2.3

[a] Excitation wavelength = 350 nm. [b] $[IrN_4C_2]^+$ was dissolved in a H_2O/CH_3CN (90/10) mixture because of its low solubility in water. [c] The quantum yield (±5%) was measured under air using $[Ru(bpy)_3]^{2+}$ as a reference; ϕ_{ref} = 0.028 in CH_3CN,[18] λ_{Exc} = 420 nm, and 293 K. [d] Radiative rate constant at 298 K ($k_r = \Phi/\tau$).

Luminescence Behavior of Iridium(III) Complexes in the Presence of Deoxynucleotides. With respect to the excited-state potentials of iridium(III) complexes and the ability of some DNA bases to act as an electron donor or acceptor, a photooxidative or photoreductive electron-transfer process could be thermodynamically possible between the excited complex and some DNA building blocks (deoxynucleotides). Thanks to the ability of iridium complexes to emit in aqueous solution, monitoring the luminescence in the presence of increased concentration of a given nucleotide can be performed. It is worth mentioning that all of the experiments presented here were carried out with nucleobase concentrations far below the aggregation and self-association limit.[19] In addition, because of the poor solubility of $[IrN_4C_2]^+$ in pure water, 10% CH_3CN (v/v) was added for each experiment with deoxynucleotides. Figure 3 shows the relative emission decrease of both $[IrN_6]^{3+}$ and $[IrN_4C_2]^+$ upon increased concentrations of deoxyguanosine-5′-monophosphate (dGMP). It is striking that solely the higher-energy emission band (λ_{em} = 514 nm) for $[IrN_4C_2]^+$ is quenched, whereas the other band (λ_{em} = 682 nm) is not affected by the presence of dGMP. A linear Stern−Volmer relationship in the luminescence intensity can be obtained from these data (Figure 3, inset), suggesting that pure dynamic quenching[20] of the excited state of both $[IrN_6]^{3+}$ and $[IrN_4C_2]^+$ is occurring in the presence of dGMP.

In the presence of deoxyadenosine-5′-monophosphate (dAMP), a luminescence quenching and a decrease of the excited-state lifetime ($\tau_0/\tau > 1$) are observed only for $[IrN_6]^{3+}$. However, in that case, a negative deviation from the Stern−Volmer linear relationship in intensity is observed (Figure 4). This presumably shows that the luminescence quenching of $[IrN_6]^{3+}$ in the presence of dAMP is more complicated than a

dx.doi.org/10.1021/ic402476b | Inorg. Chem. 2014, 53, 1507−1512

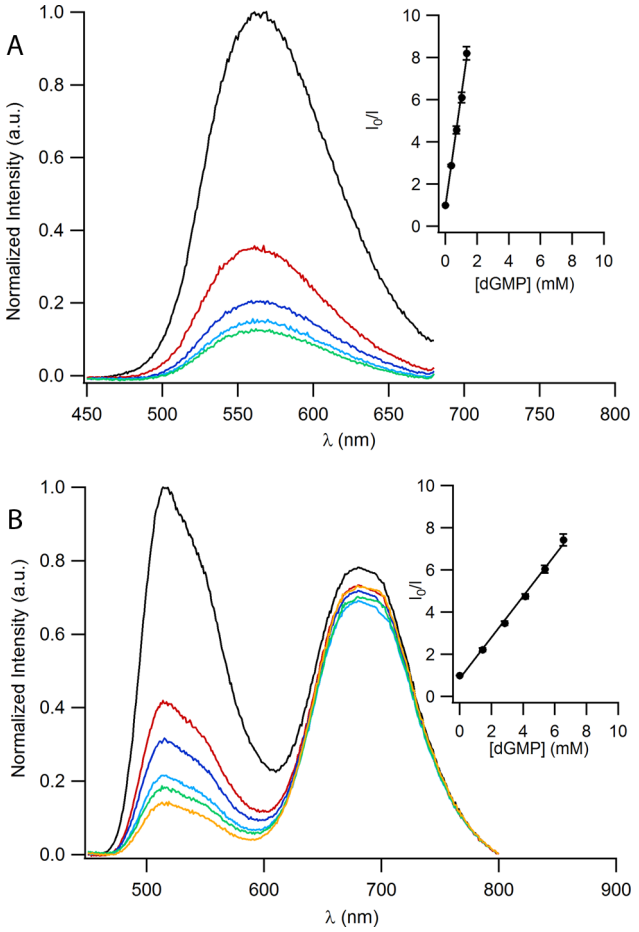

Figure 3. Luminescence spectra (λ_{exc} = 350 nm) of (a) $[IrN_6]^{3+}$ and (b) $[IrN_4C_2]^{+}$ in the presence of increased concentration of dGMP (50 mM Tris buffer, pH = 7.4, RT).[21] Inset: Stern–Volmer plots obtained upon the addition of dGMP for (a) $[IrN_6]^{3+}$ and (b) $[IrN_4C_2]^{+}$ measured at λ_{em} = 560 and 514 nm, respectively.

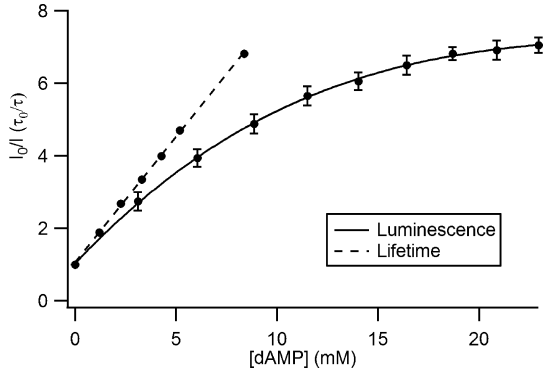

Figure 4. Stern–Volmer plots measured using the excited-state luminescence lifetime (dashed line) and luminescence intensity (solid line) of $[IrN_6]^{3+}$ upon increased concentration of dAMP (50 mM Tris buffer, pH = 7.4, RT) at λ_{em} = 560 nm (λ_{exc} = 350 nm).

simple dynamic diffusion between the excited complex and dAMP monomers.[20] The addition of dCMP or dTMP to $[IrN_6]^{3+}$ or $[IrN_4C_2]^{+}$ did not affect their luminescence behavior, excluding thus any photoinduced process involving these nucleobases.

Luminescence Behavior of $[IrN_6]^{3+}$ in the Presence of Polynucleotides. Because of the relatively low solubility of $[IrN_4C_2]^{+}$ in aqueous buffer, we have decided to limit our study of the influence of polynucleotides on the spectroscopic properties of the complex to $[IrN_6]^{3+}$.

Although no significant change in the absorption spectra of $[IrN_6]^{3+}$ is observed when interacting with the polynucleotide, its luminescence is dramatically altered. Figure 5 shows the

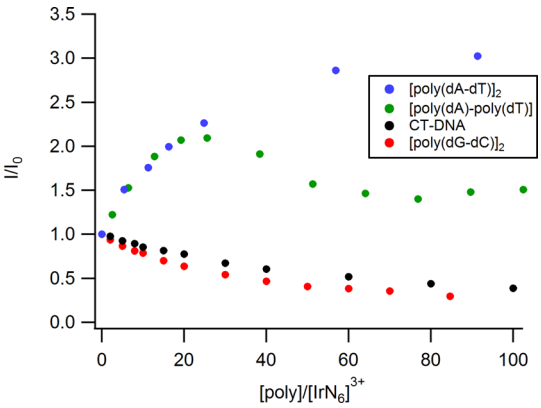

Figure 5. Relative luminescence intensity of $[IrN_6]^{3+}$ measured at λ_{em} = 560 nm in the presence of increased concentrations of [poly(dA-dT)] $_2$ (blue circle), [poly(dA)-poly(dT)] (green circle), CT-DNA (black circle), and $[poly(dG-dC)]_2$ (red circles). All of the measurements were performed with a constant complex concentration of 32 μM in a 50 mM Tris-HCl buffer aqueous solution (pH = 7.4) with 50 mM NaCl (λ_{exc} = 350 nm).

relative luminescence intensity changes I/I_0 for $[IrN_6]^{3+}$ upon the addition of selected polynucleotides. Two distinct behaviors are observed. In the presence of GC base pairs containing polynucleotides (i.e., $[poly(dG\text{-}dC)_2]$, 100% GC base pairs; CT-DNA, 42% GC base pairs[22]), a luminescence quenching is observed. In contrast, in the presence of AT base pairs containing polynucleotides (i.e., $[poly(dA\text{-}dT)_2]$ or [poly(dA)-poly(dT)], 100% AT base pairs), a somewhat more complex behavior is observed with a strong luminescence increase followed by a plateau value of $I/I_0 \approx 3$ for $[poly(dA\text{-}dT)_2]$ or followed by a decrease for [poly(dA)-poly(dT)].

DISCUSSION

Photophysics of the Complexes Alone in Solution. Iridium(III) complexes are well-known in the literature for their rich photophysics and photochemistry. Indeed, because of a strong spin–orbit coupling and an important influence of the ancillary ligands, a mixture of different excited states usually participates in the radiative deactivation of the complex. In the case of $[Ir(tpy)_2]^{3+}$ and parent compounds, it has been shown that the emission arises from a ligand-centered (^{3}LC) excited state, with a small but nonnegligible contribution of a metal-to-ligand charge-transfer (^{3}MLCT) excited state.[16]

For $[IrN_6]^{3+}$, a change in the solvent polarity (i.e., from CH_3CN to water) does not influence the emission maximum, in agreement with a ^{3}LC excited state. However, the luminescence at room temperature in a polar fluid solvent is unstructured, decays in about 1 μs, and is blue-shifted at 77 K (Table 2), which is more in favor of a ^{3}MLCT excited state. In addition, the k_r value ($\approx 10^3$ s^{-1}) is relatively high, and usually such values are much smaller for pure ^{3}LC states.[23] Therefore, we propose that the lowest excited state in $[IrN_6]^{3+}$ corresponds to a ^{3}LC centered on the electron-poorest ligand,

dx.doi.org/10.1021/ic402476b | Inorg. Chem. 2014, 53, 1507–1512

i.e., $^3[\pi \rightarrow \pi^*(4'\text{-COOH-Phtpy})]$, mixed with some ^{3}MLCT character, $^3[d\pi(\text{Ir}) \rightarrow \pi^*(4'\text{-COOH-Phtpy})]$.

In contrast, the cyclometalated compound $[\mathbf{IrN_4C_2}]^+$ displays a different photophysical behavior. Compared to $[\mathbf{IrN_6}]^{3+}$, the absorption is shifted to the red, in agreement with the greater donating ability of the cyclometalated ligand. In addition, a dual-band emission is observed. According to experimental[24] and theoretical[25] data, iridium(III) complexes made from terdentate cyclometalated ligands usually have an emitting state corresponding to a ligand-to-ligand charge transfer (LLCT), often combined with other ^{3}LC/^{3}MLCT excited states.

In the case of $[\mathbf{IrN_4C_2}]^+$, the emission at $\lambda_{em} \approx 520$ nm is similar to that of $[\mathbf{IrN_6}]^{3+}$ described above. Therefore, we ascribe this transition to a mixture ^{3}LC/^{3}MLCT, i.e., $^3[d\pi(\text{Ir}) \rightarrow \pi^*(4'\text{-COOH-Phtpy})$ and $\pi(4'\text{-COOH-Phtpy}) \rightarrow \pi^*(4'\text{-COOH-Phtpy})]$. The most bathochromic band ($\lambda_{em} = 697$ nm) is believed to correspond to a ^{3}LLCT, i.e., ^{3}[cyclometalated iridium fragment (Ir−C^N^C) $\rightarrow \pi^*(4'\text{-COOH-Phtpy})]$. Indeed, the emission at 77 K is poorly resolved, in agreement with a CT process.[23] Moreover, the addition of protons (e.g., 2 M HNO_3; Figure S4 in the SI) in the solution leads to a complete disappearance of this ^{3}LLCT emission, probably arising from protonation of the −OMe group, hence inhibiting any CT processes involving the electron-donating Ir−C^N^C fragment.

Photochemical Behavior in the Presence of Mono- and Polynucleotides. Although the total emission of $[\mathbf{IrN_6}]^{3+}$ is quenched in the presence of a G unit, solely one emission band of $[\mathbf{IrN_4C_2}]^+$ undergoes a quenching process upon the addition of GMP (Figure 3b). On the basis of thermodynamic considerations, this luminescence quenching for both complexes could be ascribed to a photoinduced electron-transfer process from the G unit to the excited complexes (eqs 1 and 2).

$$[IrN_6]^{3+}* + G \rightarrow [IrN_6]^{2+} + G^{\bullet+} \quad (1)$$

$$[IrN_4C_2]^{+}* + G \rightarrow [IrN_4C_2] + G^{\bullet+} \quad (2)$$

Indeed, although the G oxidation potential has been debated for a long time in the literature, it is generally accepted that E_{ox} of isolated G is close to +1.10 V vs Ag/AgCl and even less positive when stacked to other G units (E_{ox}poly(dG-dC)$_2$] < +0.85 V vs Ag/AgCl).[26] Considering the oxidation power of the excited state of $[\mathbf{IrN_6}]^{3+}$ and using the empirical Rehm−Weller equation,[27] it is expected that process (1) will be exergonic by about 0.3 eV.[17] In the case of $[\mathbf{IrN_4C_2}]^+$, solely the most energetic emission band ($\lambda_{em} = 514$ nm) is quenched via a photoreductive electron transfer (eq 2), favored by less than 0.1 eV based on thermodynamic assumptions. The low oxidizing power of the less energetic excited state (LLCT) does not allow any G oxidation. Efficient quenching in the presence of G units is also in agreement with the high value of the quenching rate constant (k_q) obtained from the Stern−Volmer plot of $[\mathbf{IrN_6}]^{3+}$ and $[\mathbf{IrN_4C_2}]^+$ with dGMP (vide supra; Stern−Volmer plots, Figure 3, inset; $k_q = 3.9 \times 10^9$ M^{-1} s^{-1} for $[\mathbf{IrN_6}]^{3+}$ and 5.3×10^8 M^{-1} s^{-1} for $[\mathbf{IrN_4C_2}]^+$), both close to the diffusion limit.

The behavior of $[\mathbf{IrN_6}]^{3+}$ in the presence of A units is less common. The emission lifetimes dramatically decrease upon the addition of dAMP, evidencing an efficient quenching of the excited state with $k_q = 5.3 \times 10^8$ M^{-1} s^{-1} (Figure 4). However, a deviation from the linearity of the Stern−Volmer relationship for the emission intensity (I_0/I) is observed (Figure 4). This usually arises when static quenching is operative, but in that particular case, an upward curvature is observed. Instead, for $[\mathbf{IrN_6}]^{3+}$, a downward curvature indicates that other processes have to be taken into account. A similar behavior has been reported in the literature for the fluorescence quenching of doxorubicin in the presence of AMP.[28] Two conformers (i.e., with one or two intramolecular hydrogen-bonded hydrophenolic moieties) of doxorubicin in the ground state with different accessibility to the quencher were shown to be responsible for the emission quenching behavior. In the present case, (de)protonation of the carboxylic acid moiety could generate two ground states with a different quenching constant by dAMP. Experiments at different pH values in buffered aqueous solution showed that the proton concentration of the medium has only a small influence on the quenching behavior (Figure S5 in the SI). Moreover, converting the acid function into an ester has no effect (Figures S6 and S7 in the SI). Therefore, it is likely that the behavior of $[\mathbf{IrN_6}]^{3+}$ in the presence of dAMP originates from the complex mixture of excited states participating in the emission, with each state being successively reductively quenched by dAMP with different rate constants. In the presence of oligonucleotides, the change of luminescence of $[\mathbf{IrN_6}]^{3+}$ strongly depends on the nature of the nucleobase content. In agreement with the behavior observed in the presence of dGMP, quenching of excited $[\mathbf{IrN_6}]^{3+}$ with [poly(dG-dC)]$_2$ or CT-DNA would arise from the photoinduced electron-transfer process from a G unit of the polynucleotide to the excited complex, hence generating oxidative damage within the DNA double helix. The plateau value, reflecting the quenching efficiency, does not seem to depend on the percentage of GC of the polynucleotide, in contrast to G photooxidizing ruthenium(II) complexes.[22] This shows that the quenching of the excited state of $[\mathbf{IrN_6}]^{3+}$ is highly efficient, in agreement with its very high oxidation power when irradiated by light.

In contrast, in the presence of adenine-rich polynucleotides such as [poly(dA-dT)]$_2$ or [poly(dA)-poly(dT)], a luminescence increase is recorded, in spite of the sufficiently reducing power of A for quenching the excited state of $[\mathbf{IrN_6}]^{3+}$ (vide supra; Figure 4). The luminescence of the complex in the presence of these specific polynucleotides probably originates from two antagonist processes: (i) protection of the complex from the solvent molecules and from oxygen by the DNA hydrophobic environment (via intercalation or groove binding, for instance), resulting in a luminescence increase, and (ii) quenching by the A moieties, resulting in a luminescence decrease. In the case of the alternating copolymeric [poly(dA-dT)]$_2$, the luminescence enhancement is monotonic, reflecting a constant involvement of both processes at any [poly]/[IrN$_6$]$^{3+}$ ratio, with the protection effect being predominant. For the homopolymeric [poly(dA)-poly(dT)], a different behavior is observed; this could originate from a different type of interaction with the double helix, depending on the polynucleotide loading level by the complex (Figure 5). Thus, because of these structural changes, at [poly]/[IrN$_6$]$^{3+}$ > 40, the quenching by the A units would become predominant compared to their protection, which would account for the inflection observed in the titration curve.

■ CONCLUSION

We managed to synthesize two new bis-terdendate iridium(III) complexes. Both have been obtained thanks to successive addition of the ligands on the metal center. The spectroscopic

dx.doi.org/10.1021/ic402476b | Inorg. Chem. 2014, 53, 1507−1512

and electrochemical data revealed that several excited states contribute to the overall luminescence. Oxidative quenching of the $[IrN_6]^{3+}$ emission in the presence of dGMP or dAMP confirms the high oxidizing ability of the excited complex. The behavior of $[IrN_4C_2]^+$ is less common. Indeed, a selective quenching of the most energetic excited state is observed in the presence of dGMP. No quenching in the presence of dTMP or dCMP was evidenced for both complexes. This shows that these two iridium(III) complexes are not sufficiently reducing (or oxidizing) in their excited state to reduce (or oxidize) thymine or cytosine derivatives. Therefore, selective oxidative electron-transfer processes involving DNA purine bases can be triggered upon irradiation of these new iridium(III) complexes.

■ ASSOCIATED CONTENT

Ⓢ Supporting Information

Synthetic details and spectroscopic properties of esterified $[IrN_6]^{3+}$, luminescence experiments in the presence of dGMP for esterified $[IrN_6]^{3+}$, luminescence experiments in the presence of dAMP at different pH values for $[IrN_6]^{3+}$, ^1H NMR spectra and HRMS data for all complexes, disappearance of luminescence of $[IrN_4C_2]^+$ upon the addition of HNO_3, and cyclic voltammograms. This material is available free of charge via the Internet at http://pubs.acs.org.

■ AUTHOR INFORMATION

Corresponding Author

*E-mail: Benjamin.Elias@uclouvain.be.

Present Address

†A.K-D.: Service de Chimie Organique et Photochimie, Université libre de Bruxelles, CP160/08, 50 Av F. D. Roosevelt, B-1050 Brussels, Belgium.

Author Contributions

All authors have given approval to the final version of the manuscript.

Notes

The authors declare no competing financial interest.

■ ACKNOWLEDGMENTS

The authors gratefully acknowledge the Fonds National pour la Recherche Scientifique (F.R.S.-F.N.R.S.), the Fonds pour la Formation à la Recherche dans l'Industrie et dans l'Agriculture (F.R.I.A.), the Région Wallonne, the Université catholique de Louvain, and the Prix Pierre et Colette Bauchau for financial support. We are also grateful to L. Marcélis and L. Troian-Gautier for their scientific help.

■ REFERENCES

(1) (a) Du, P.; Knowles, K.; Eisenberg, R. *J. Am. Chem. Soc.* **2008**, *130*, 12576−12577. (b) DiSalle, B. F.; Bernhard, S. *J. Am. Chem. Soc.* **2011**, *133*, 11819−11821. (c) Ozawa, H.; Sakai, K. *Coord. Chem. Rev.* **2007**, *251*, 2753−2766.

(2) (a) Gasser, G.; Ott, I.; Metzler-Nolte, N. *J. Med. Chem.* **2011**, *54*, 3−25. (b) Le Gac, S.; Rickling, S.; Gerbaux, P.; Defrancq, E.; Moucheron, C.; Kirsch-De Mesmaeker, A. *Angew. Chem., Int. Ed.* **2009**, *48*, 1122−1125. (c) Gianferrara, T.; Bratsos, I.; Alessio, E. *Dalton Trans.* **2009**, *37*, 7588−7598.

(3) (a) Erkkila, K. E.; Odom, D. T.; Barton, J. K. *Chem. Rev.* **1999**, *99*, 2777−2796. (b) Elias, B.; Kirsch-De Mesmaeker, A. *Coord. Chem. Rev.* **2006**, *250*, 1627−1641. (c) McKinley, A. W.; Lincoln, P.; Tuite, E. M. *Coord. Chem. Rev.* **2011**, *255*, 2676−2692. (d) Moucheron, C. *New J. Chem.* **2009**, *33*, 235−245. (e) Smith, J. A.; George, M. W.; Kelly, J. M. *Coord. Chem. Rev.* **2011**, *255*, 2666−2675. (f) Lo, K. K-W.; Zhang, K. Y. *RSC Adv.* **2012**, *2*, 12069−12083.

(4) (a) Dixon, I. M.; Collin, J.-P.; Sauvage, J.-P.; Flamigni, L.; Encinas, S.; Barigelletti, F. *Chem. Soc. Rev.* **2000**, *29*, 385−391. (b) Flamigni, L.; Collin, J.-P.; Sauvage, J.-P. *Acc. Chem. Res.* **2008**, *41*, 857−871. (c) Baranoff, E.; Collin, J.-P.; Flamigni, L.; Sauvage, J.-P. *Chem. Soc. Rev.* **2004**, *33*, 147−155.

(5) (a) Zhao, Q.; Liu, S.; Shi, M.; Li, F.; Jing, H.; Yi, T.; Huang, C. *Organometallics* **2007**, *26*, 5922−5930. (b) Lo, K. K-W.; Louie, M.-W.; Zhang, K. Y. *Coord. Chem. Rev.* **2010**, *254*, 2603−2622.

(6) (a) Elias, B.; Genereux, J. C.; Barton, J. K. *Angew. Chem., Int. Ed.* **2008**, *47*, 9067−9070. (b) Shao, F.; Elias, B.; Barton, J. K. *Inorg. Chem.* **2007**, *46*, 10187−10199. (c) Shao, F.; Barton, J. K. *J. Am. Chem. Soc.* **2007**, *129*, 14733−14738.

(7) Campagna, S.; Cavazzini, M.; Cusumano, M.; Di Pietro, M. L.; Giannetto, A.; Puntoriero, F.; Quici, S. *Inorg. Chem.* **2011**, *50*, 10667−10672.

(8) Wang, J.; Hanan, G. S. *Synlett* **2005**, *8*, 1251−1254.

(9) Shinpuku, Y.; Inui, F.; Nakai, M.; Nakabayashi, Y. *J. Photochem. Photobiol. A* **2011**, *222*, 203−209.

(10) Goldstein, D. C.; Chen, Y. Y.; Schmidt, T. W.; Bhadbhade, M.; Thordarson, P. *Dalton Trans.* **2011**, *40*, 2053−2061.

(11) Adib, M.; Tahermansouri, H.; Koloogani, S. A.; Mohammadi, B.; Bijanzadehb, H. R. *Tetrahedron Lett.* **2006**, *47*, 5957−5960.

(12) Felsenfeld, G.; Hirschman, S. Z. *J. Mol. Biol.* **1965**, *13*, 407−427.

(13) Inman, R. B.; Baldwin, R. L. *J. Mol. Biol.* **1962**, 172−184.

(14) Cui, T.; Wei, S.; Brew, K.; Leng, F. *J. Mol. Biol.* **2005**, *352*, 629−645.

(15) Wells, R. D.; Larso, J. E.; Grant, R. C.; Shortle, B. E.; Cantor, C. R. *J. Mol. Biol.* **1970**, *54*, 465−497.

(16) Collin, J.-P.; Dixon, I. M.; Sauvage, J.-P.; Williams, G. A.; Barigelletti, F.; Flamigni, L. *J. Am. Chem. Soc.* **1999**, *121*, 5009−5016.

(17) $\Delta G_{ET} = E_{ox}(\text{deoxynucleobase}) - E_{red}^*$, where E_{ox}(deoxynucleobase) is the oxidation potential of a selected deoxynucleobase and E_{red}^* is the reduction potential of $[IrN_6]^{3+}$ and $[IrN_4C_2]^+$ in their excited states. Therefore, we have obtained $\Delta G_{ET} = 1.10 - 1.38 = -0.28$ eV and $\Delta G_{ET} = 1.10 - 1.12 = -0.02$ eV respectively for $[IrN_6]^{3+}$ and $[IrN_4C_2]^+$.

(18) Juris, A.; Balzani, V.; Barigelletti, F.; Campagna, S.; Belser, P.; Von Zelewsky, A. *Coord. Chem. Rev.* **1988**, *84*, 85−277.

(19) Wong, A.; Ida, R.; Spindler, L.; Wu, G. *J. Am. Chem. Soc.* **2005**, *127*, 6990−6998.

(20) Balzani, V.; Scandola, F. *Supramolecular Photochemistry*; Ellis Horwood: Chichester, U.K., 1991.

(21) The low solubility of $[IrN_4C_2]^+$ prevents its dissolution in a pure aqueous Tris buffer. Therefore, 10% of acetonitrile has been added to the buffer in order to have complete dissolution of the complex.

(22) Ortmans, I.; Elias, B.; Kelly, J. M.; Moucheron, C.; Kirsch-De Mesmaeker, A. *Dalton Trans.* **2004**, *4*, 668−676.

(23) Flamigni, L.; Barbieri, A.; Sabatini, C.; Ventura, B.; Barigelletti, F. *Top. Curr. Chem.* **2007**, *281*, 143−203.

(24) Polson, M.; Fracasso, S.; Bertolasi, V.; Ravaglia, M.; Scandola, F. *Inorg. Chem.* **2004**, *43*, 1950−1956.

(25) Polson, M.; Ravaglia, M.; Fracasso, S.; Garavelli, M.; Scandola, F. *Inorg. Chem.* **2005**, *44*, 1282−1289.

(26) Steenken, S.; Jovanovics, V. *J. Am. Chem. Soc.* **1997**, *119*, 617−618.

(27) Rehm, D.; Weller, A. *Ber. Bunsen Ges.* **1969**, *73*, 834−839.

(28) Htun, T. *J. Fluoresc.* **2004**, *14*, 217−222.